

UDC: 538.9 Condensed matter Physics, Solid state Physics, Theoretical Condensed matter Physics

TEMPERATURE DEPENDENCE OF GAS SENSITIVITY OF FERRIC OXIDE THIN FILMS IN CO₂ GAS, ACETONE, ETHANOL AND METHANOL VAPORS

P. Samarasekara ¹, M.S.P.K. Gunasinghe ¹, P.G.D.C.K. Karunarathna ², H.T.D.S. Madusanka ² and C.A.N. Fernando ²

¹Department of Physics, University of Peradeniya, Peradeniya, Sri Lanka

²Department of Nano Science Technology, Wayamba University of Sri Lanka, Kuliyaipitiya, Sri Lanka

Abstract

Thin films of ferric oxide (α -Fe₂O₃) were synthesized by the doctor blade method starting from a solution of iron acetate and PEG binder. The samples were subsequently annealed at 500 °C in air for one hour. The surface morphology of the samples was determined by SEM. The samples consist of closely packed spherical particles in the size of about 150 nm. The gas sensitivity, recovery time and response time of the α -Fe₂O₃ samples were measured in CO₂ gas, acetone, ethanol and methanol vapors at room temperature. Then the same parameters of the α -Fe₂O₃ samples in CO₂ gas were measured at different operating temperatures from the room temperature to 200 °C. The α -Fe₂O₃ samples indicated the highest sensitivity of 66.91% in CO₂ gas at the room temperature compared with the other three vapors. This is one of the highest gas sensitivities reported for the α -Fe₂O₃ thin films in CO₂ gas. However, the best recovery and response times of the samples were found in the ethanol vapor at the room temperature. The gas sensitivity of the samples in CO₂ gas increased with the operating temperature up to 170 °C, and then gradually decreased with the operating temperature. The gas sensitivity of α -Fe₂O₃ samples in CO₂ gas increases by a factor of 1.17 at 170 °C, compared with the gas sensitivity in CO₂ gas at the room temperature. In addition, the best response and recovery times in CO₂ gas were observed at 170 °C.

Keywords: Doctor blade method, gas sensors, gas sensitivity, operating temperature

1. Introduction:

Iron oxides have different stoichiometries such as FeO, Fe₂O₃ and Fe₃O₄. Iron oxide finds potential applications in photodynamic therapy, agriculture applications, magnetic recording, magnetic memory devices, gas sensors and biosensors. Thin films of γ -Fe₂O₃ have been synthesized on glass substrates at 350 °C, and thin films of α -Fe₂O₃ have been deposited between 400 and 500 °C by gas phase deposition [1]. Thin films of iron oxide have been fabricated by both post-oxidation of pure Fe ultra-thin films and by evaporating Fe onto the MO substrates [2]. Colored iron oxide thin films have been grown by Sol-gel technique [3]. Iron oxide thin films have been synthesized on fused quartz substrate using simple metal organic deposition from Fe-(III) acetylacetonate as the organic precursor [4]. Fe₃O₄ thin films have been sputtered using a target consisting of a mixture of Fe₃O₄ and Fe₂O₃ onto Si and glass substrates [5]. Also thin films of hematite have been synthesized using pulsed laser depositions (PLD) [6]. Fe₂O₃ thin film gas sensor sensitive to organic vapors and hydrogen gas have been synthesized using cathodic sputtering [7]. Fe₂O₃ gas sensing films have been fabricated by normal pressure chemical vapor deposition to detect acetone and alcohol [8]. Fe₂O₃ thick film sensors have been applied to detect CH₄, H₂ and NH₃ [9]. Hollow balls of nano Fe₂O₃ have been employed to detect dimethyl methylphosphonate at room temperature [10]. It is possible to control the gas sensing properties of hematite nanocrystals by controlling the

morphology [11]. Gas sensing properties of p-type α -Fe₂O₃ polyhedral particles have been investigated [12]. NaBH₄ added α -Fe₂O₃ microparticles with size of 1-10 μ m have been prepared [13].

Thin films have been synthesized using chemical vapor deposition, sputtering techniques and evaporation techniques incorporated with vacuum previously [14, 15, 16, 17]. Compared to the expensive techniques with vacuum, doctor blade method was found to be lower in cost and faster. The band gap of semiconductor particles can be determined using electrical conductivity measurements too [18]. Iron oxide belongs to the category of ferrimagnetic materials. Magnetic properties of ferromagnetic and ferrite thin films have been investigated using the second and third order perturbed Heisenberg Hamiltonian by us [19-23]. Applications of gas sensors have been presented in many manuscripts [24-31]. In this manuscript, we report the gas sensing properties of α -Fe₂O₃ thin films in CO₂ gas and many vapors at different operating temperatures.

2. Experimental:

Initially 1.5002 g of iron acetate nanoparticles was dissolved in 10 ml of water to prepare a solution of 2 M. Then the solution was stirred on a magnetic stirrer at 600 rpm for 1 hour to mix the solution. The solution was placed inside a furnace at 500 °C for two hours with 10 °C min⁻¹ heating rate. Then 0.0503 g of polyethylene glycol (PEG) was mixed with 8 ml of water. It was placed on a magnetic stirrer and stirred at 45 °C temperature for 15 minutes. Thereafter, PEG solution (2 ml) was added to iron acetate solution, and a few drops of ethanol was added to it. Then the solution was placed on the magnetic stirrer, and it was stirred at 600 rpm for two hours at 50 °C temperature. Finally the prepared iron acetate-PEG solution was applied to a conductive FTO glass plate or a normal non-conductive glass plate to prepare α -Fe₂O₃ thin films using a doctor blade method. Thin films grown on conductive FTO glass plates were used for gas sensitivity measurements. FTO glass plates with the area of 3.5 cm x 2 cm were used. A strip of 0.6 cm x 2 cm was scratched in the middle of the conducting side on FTO. Then glass slides were well cleaned using ethanol. Because the scratched glass slide is used to fabricate the gas sensor, only the α -Fe₂O₃ layer conducts the electric current. In the doctor blade method, cello tapes glued to the edges of the glass plates were used to control the thickness. First the prepared samples were heated on hot plate at 50 °C temperature for 1 hour. Then the thin films were cooled down in normal air for 2 hours. Thereafter, they were placed inside the oven at 150 °C temperature for 1 hour to remove excess oxygen and water vapor from the sample. Next the thin films were annealed in the furnace at 500 °C for one hour in air to crystallize the phase of α -Fe₂O₃

α -Fe₂O₃ thin films were connected to a 5 V power supply for 6 hours to stabilize the sensor. Gold coated electrodes and wires were used for all the connections. The sensor electrode wires were connected to a Keithley 6400 source meter unit to measure the current carrying through the gas sensor. Then the Keithley 6400 source meter was adjusted for current measuring mode, and 5.0 V was applied to the gas sensor. Next the measured time period was adjusted to 5000 s, and "AUTO LAB" measuring unit was switched on to measure the current carrying through the gas sensor. After stabilizing the current, some known amount of CO₂ gas (1000 ppm) was injected in to the glass chamber using a syringe. Then electric current increased and reached the saturated value of the current, and this saturated current was noted down. The time taken to reach the saturated current was also measured. This is called the respond time. Thereafter, normal atmospheric air was pumped in to the glass chamber to remove the CO₂ gas, and the air was pumped continuously in to the glass chamber until the current reading returned to initial stable value. The time taken to reach the initial stable value was also measured. This is called the recovery time. Then the air pump was switched off and, few minutes were given to stabilize the gas sensor. Thereafter, CO₂ gas was introduced again to the gas chamber, and above procedure was repeated to obtain another current variation cycle. This procedure was repeated for the gas sensors prepared with the binder (PEG), and the current response variation was compared. The same procedure was repeated to measure gas sensitivity of iron oxide thin films in methanol, ethanol and acetone vapors.

The gas sensitivity was measured at different operating temperatures as follows. The room temperature was found using a thermocouple connected to the gas sensor. Then the gas sensor was heated to temperature of 60 °C using a coil heater connected to a power supply. Few minutes were given to stabilize the initial current. Then above procedure was repeated to measure the gas sensitivity in different gases and vapors. Similarly the gas sensitivity, recovery time and response time were measured at operating temperatures of 90, 120, 150, 180 and 210 °C. Surface morphology and particle size were determined using Zeiss Evols 15 scanning electron microscope (SEM).

3. Results and Discussion:

All the samples described in this section were prepared with PEG binder by the doctor blade method. The samples were subsequently annealed at 500 °C for one hour in air to crystallize the single phase of α -Fe₂O₃. According to the XRD, FTIR and UV-visible data, the single phase of α -Fe₂O₃ could be crystallized under these conditions [32]. Figure 1 shows the SEM micrograph of the α -Fe₂O₃ thin films sample. Fe₂O₃ spherical shape particles can be observed. Particles are closely packed without any voids. The sample seems to be uniform. Therefore, SEM image observation reveals that prepared α -Fe₂O₃ products consists of spherical grains with diameter around 150 nm.

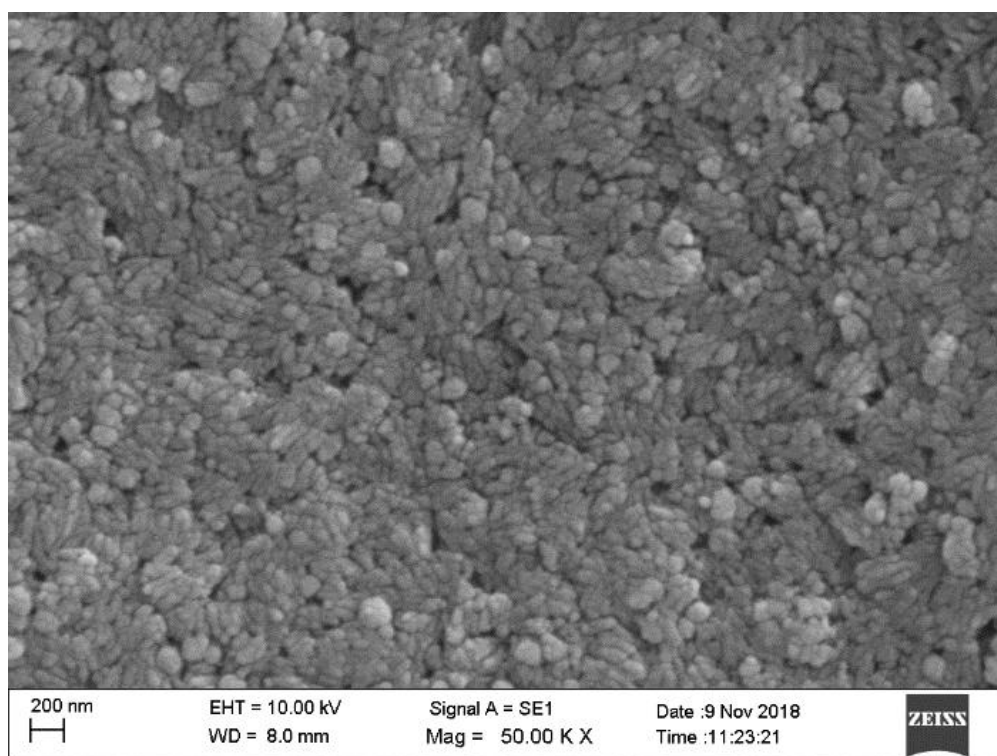


Figure 1: SEM image of the α -Fe₂O₃ thin film prepared by the doctor blade method.

Figure 2 represents the curves of current, resistance and gas sensitivity versus time for CO₂ gas, acetone, ethanol and methanol vapors at the room temperature (28 °C). The current (I) in μ A range was measured by AUTO LAB unit. Because 5V is applied to the sample, the resistance was calculated using $R=5/I$. The gas sensitivity of α -Fe₂O₃ was measured at 1000 ppm gas or vapor amount in the gas chamber. The gas sensitivity was calculated using the following equation.

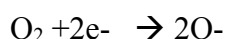
$$\text{Gas sensitivity} = \frac{|R_g - R_a|}{R_a} \times 100\%$$

Here R_g is the saturated value of the resistance of the sample after the gas is completely absorbed by the sample, and R_a is the saturated value of the resistance after the gas is completely released by the sample.

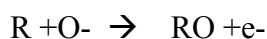
According to the curves, CO₂ gas indicates the maximum gas sensitivity of 66.91% at the room temperature. The response and recovery times of α -Fe₂O₃ thin film in CO₂ gas are 819 and 619 s, respectively. Gas sensitivity of α -Fe₂O₃ thin film in acetone vapor is 56.43%, and response and recovery times are 310 and 344 s, respectively. For ethanol vapor, the gas sensitivity is 38.27%, and response and recovery times are 69 and 86 s, respectively. The lowest gas sensitivity at room temperature was observed in methanol vapor, and it is 32.04%. The response and recovery times in methanol vapor are 665 and 494 s, respectively. CO₂ gas takes the maximum time to respond to the gas sensor. In the presence of ethanol vapor, α -Fe₂O₃ gas sensor responses quickly. But the gas sensitivity value is low in ethanol vapor. According to the gas sensitivity measurements, α -Fe₂O₃ gas sensor can be used to detect CO₂ gas, acetone, ethanol and methanol vapors, however, it is more suitable to detect CO₂ gas.

The resistance of α -Fe₂O₃ thin film decreases after absorbing CO₂ gas, acetone and ethanol vapors. However, the resistance of α -Fe₂O₃ thin film increases after absorbing methanol vapor. This is related to the chemisorption and physisorption processes. Chemisorption is a kind of adsorption which involves a chemical reaction between the surface and the adsorbate. New chemical bonds are generated at the adsorbent surface. Physisorption is the physical bonding of gas molecules to the surface of a solid or liquid that the gas comes into contact with at low temperatures. This occurs due to Van der Waals forces.

Atmospheric O₂ molecules are physisorbed on the surface site, and become ionized by taking an electron from the conduction band as following. This leads to an increase in resistance of the sensor material.



The reducing gas (R) reacts with the chemisorbed oxygen, thereby releasing an electron back to the conduction band and decreasing the resistance of the sensor material as following.



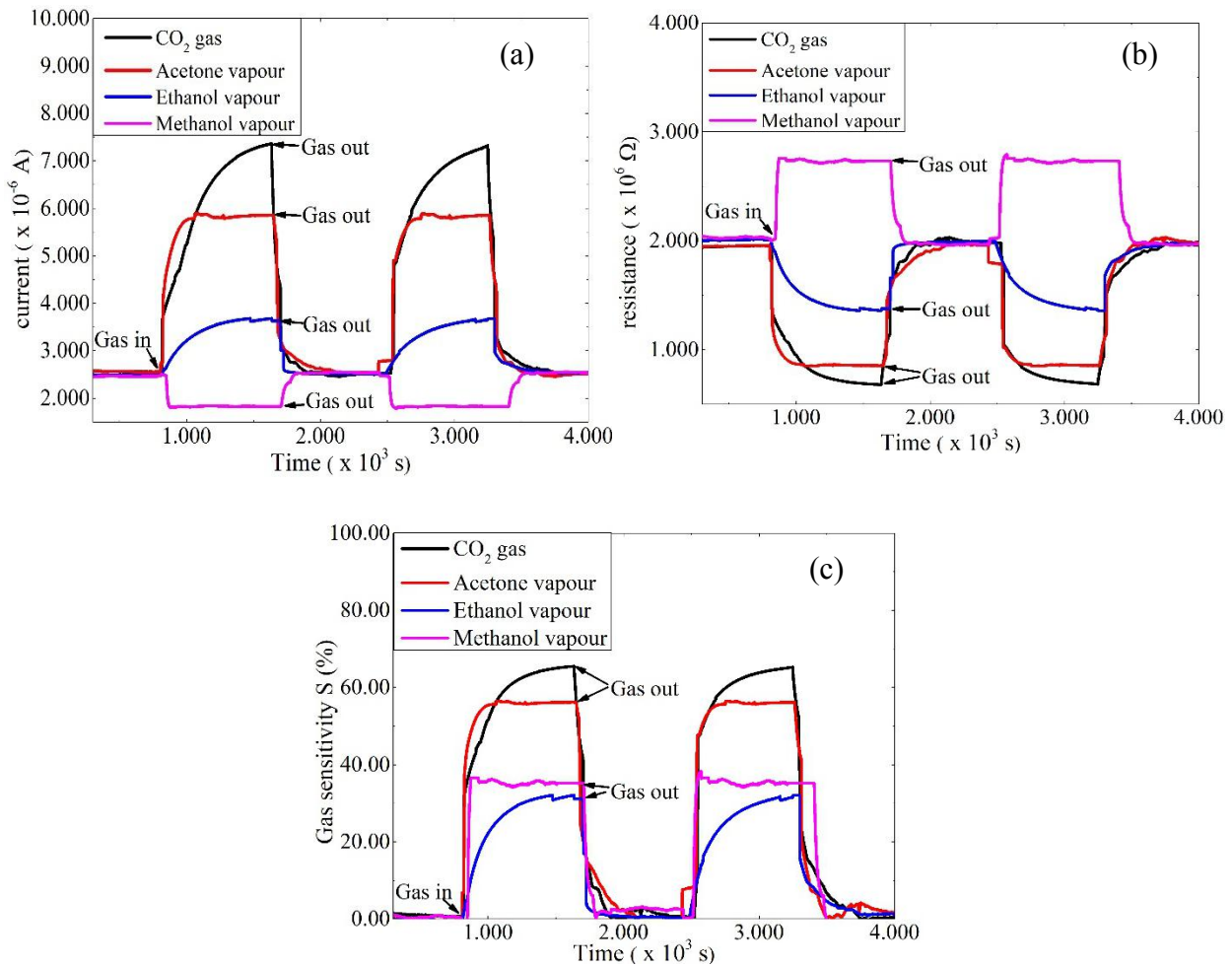


Figure 2: Graphs of current, resistance and gas sensitivity versus time for CO₂ gas, acetone, ethanol and methanol vapors.

Figure 3 shows the bar chart of the gas sensitivity for CO₂ gas, acetone, ethanol and methanol vapors at the room temperature. Table 1 represents the response time, recovery time and the gas sensitivity for CO₂ gas, acetone, ethanol and methanol vapors at the room temperature.

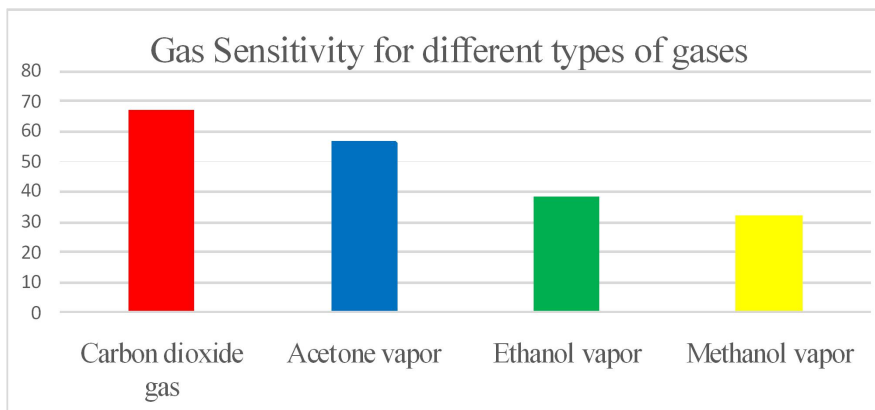


Figure 3: Bar chart of the gas sensitivity for CO₂ gas, acetone, ethanol and methanol vapors.

Table1: Response time, recovery time and the gas sensitivity for CO₂ gas, acetone, ethanol and methanol vapors.

Gas type	Response time (s)	Recovery time (s)	Gas sensitivity (%)
Carbon dioxide gas	819	619	66.91
Acetone vapor	310	344	56.43
Ethanol vapor	69	86	38.27
Methanol vapor	665	494	32.04

Figure 4 shows the variation of the current, resistance and gas sensitivity with time for 1000ppm of CO₂ gas at different temperatures. At room temperature, the gas sensitivity of CO₂ in α -Fe₂O₃ gas sensor is 66.91%. When the temperature of the gas sensor is increased, kinetic energy of atoms increases. At high kinetic energy, more electrons are excited into the conduction band, and electron density of the gas sensor becomes high. Electric field applied to the gas sensor increases the mobility of the electrons at high temperatures, and the electric current of the gas sensor increases up to a certain temperature. After a certain temperature, the collisions between conduction electrons dominate. As a result, the electric current decreases with the temperature after a particular temperature.

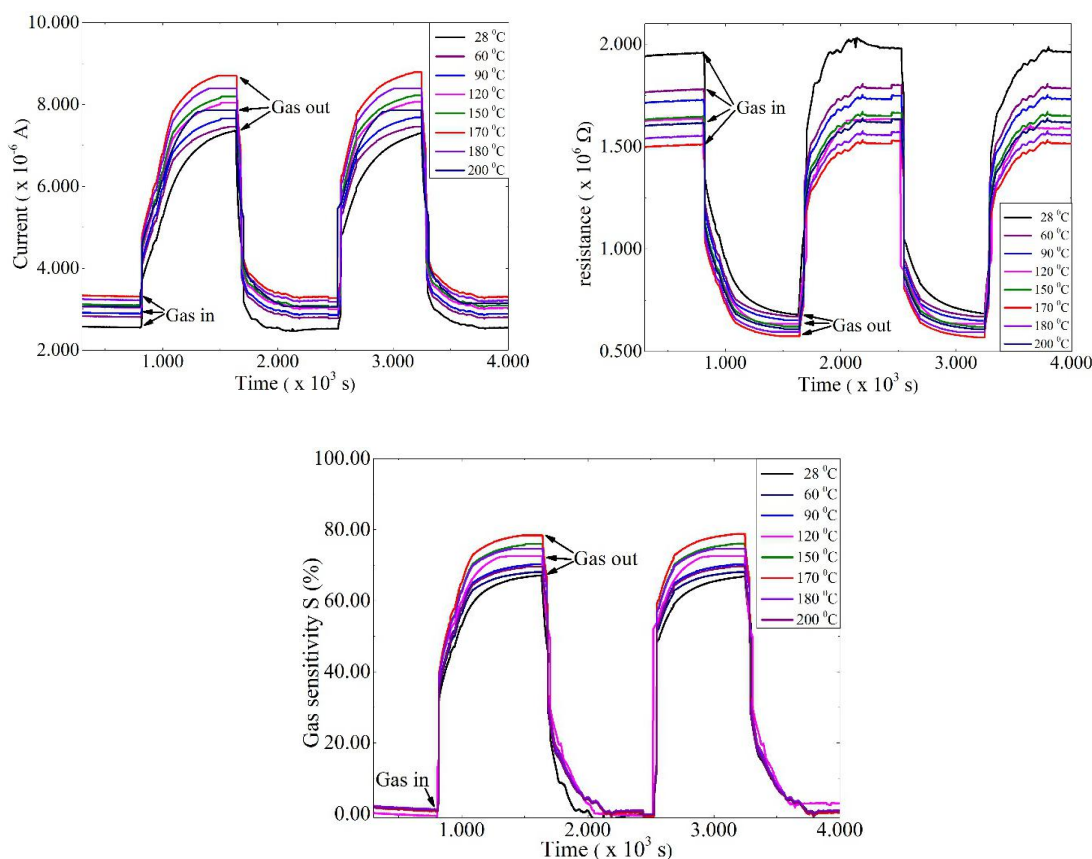


Figure 4: Variation of the current, resistance and gas sensitivity with time for CO₂ gas at different operating temperatures.

This can also be explained using the chemisorption and physisorption. The gas sensing mechanism depends on the surface reaction between chemisorbed oxygen and reducing gases. The adsorption of oxygen on the film surface has two forms: physisorption and chemisorption. At elevated temperature, chemisorption is dominant. The transition from physisorption to chemisorption needs activation energy, which can be accomplished by increasing the operating temperature. It has been observed that the amount of oxygen adsorbed on the sensor surface goes on increasing with an increase in temperature, and reaches to maximum. However, when the temperature is very high, the

oxygen atoms leave the surface of the gas sensor, and gas sensitivity decreases with further increase in the operating temperature.

Figure 5 represents the curve of gas sensitivity versus operating temperature for CO₂ gas. Table 2 shows the gas sensitivity, response time and recovery time of α -Fe₂O₃ gas sensor in CO₂ gas. The maximum gas sensitivity in CO₂ gas obtained at 170 °C temperature is 78.22%. At this temperature, the gas sensitivity increased by a factor of 1.17 compared with the gas sensitivity at the room temperature. The response and recovery times decrease when increasing the operational temperature. At room temperature, response and recovery times are 819, 619 s respectively. At 170 °C temperature, response and recovery times reach the minimum values. Gas sensors with highest sensitivity and lowest respond and recovery time are the best gas sensors. Therefore, all the properties of the α -Fe₂O₃ gas sensor can be optimized at 170 °C. The maximum sensitivity obtained for CO₂ gas by us is really larger than those obtained by some other researches [33, 34, 35]. But the response and recovery times reported in those reports for CO₂ gas are slightly better than those of our samples measured in CO₂ gas.

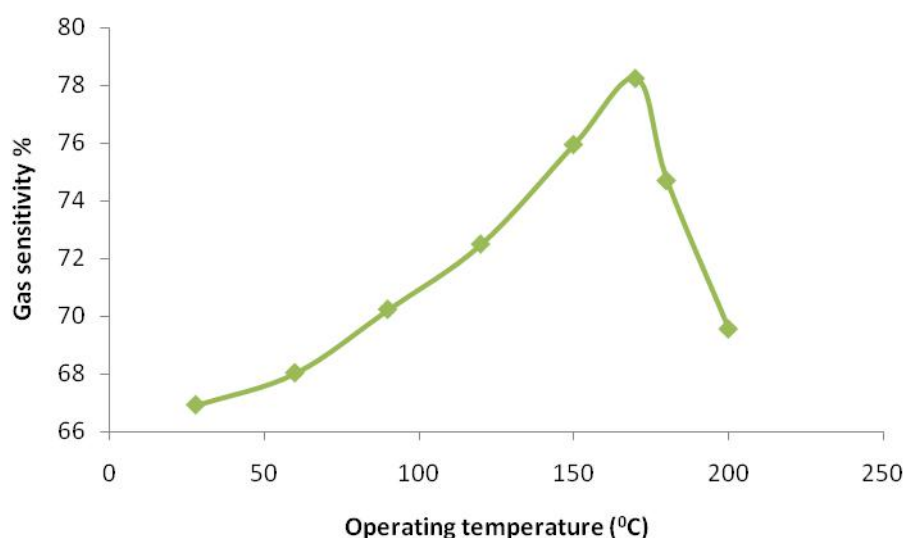


Figure 5: Curve of gas sensitivity versus operating temperature for CO₂ gas.

Table 2: Gas sensitivity, response time and recovery time of α -Fe₂O₃ gas sensor in CO₂ gas.

Operating temperature (°C)	Response time (s)	Recovery time (s)	Gas sensitivity (%)
28	819	619	66.91
60	803	606	68.02
90	792	597	70.22
120	758	563	72.48
150	723	538	75.93
170	686	511	78.22
180	743	548	74.68
200	811	605	69.54

4. Conclusion:

Gas sensitivity, response time and recovery time of α -Fe₂O₃ thin films were measured in 1000ppm of different gas species such as CO₂, acetone, ethanol and methanol vapors at the room temperature. α -Fe₂O₃ is highly sensitive to CO₂ gas compared to acetone, ethanol and methanol vapors. The gas sensitivity of α -Fe₂O₃ thin films is 66.91% in CO₂ gas. α -Fe₂O₃ indicates the lowest sensitivity of

32.04% in the methanol vapor at the room temperature. The best response time (69 s) and recovery time (86 s) can be observed in the ethanol vapor at the room temperature. The gas sensitivity, response time and recovery time of α -Fe₂O₃ thin films were measured in 1000ppm of CO₂ at different operating temperatures. The lowest sensitivity of 66.91% was observed at the room temperature, and the highest sensitivity of 78.22% was observed at 170 °C. The gas sensitivity gradually increased from the room temperature to 170 °C and then decreased with the further increase of the operating temperature. The best response time (686 s) and recovery time (511 s) were also obtained at 170 °C. The transition from physisorption to chemisorption needs activation energy, which can be accomplished by increasing the operating temperature. As a result, the gas sensitivity increases with the operating temperature. When the temperature is further increased O₂ atoms move out from the surface of the material. As a result, the gas sensitivity decreases when the temperature is further increased.

References:

1. M. Aronniemi, J. Lahtinen and P. Hautajarvi, *Surface and Interface Analysis* (2004), 36, 1004.
2. Jason S. Corneille, Jian-Wei He and D. Wayne Goodman, *Surface Science* (1995), 338(1), 211.
3. Xianhui Zhao, Changhong Li, Qiuping Liu, Yandong Duan, Junjing He, Su Liu, Hai Wang and Song Liang, *Journal of Physics: Conference Series* (2013), 419, 012033.
4. Bonamali Pal and Maheshwar Sharon, *Thin Solid Films* (2000), 379 (1-2), 83.
5. Yingguo Peng, Chando Park and David E. Laughlin, *Journal Applied Physics* (2003), 93(10), 7957.
6. C.X. Kronawitter, S.S. Mao and B.R. Antoun, *Applied Physics Letters* (2011), 98(9), 092108.
7. Karel Siroky, Jana Jiresova and Lubomir Hudec, *Thin Solid Films* (1994), 245 (1-2), 211.
8. J. Peng and C.C. Chai, *Sensors and Actuators B: Chemical* (1993), 14 (1-3), 591.
9. V.V. Malyshev, A.V. Eryshkin, E.A. Koltypin, A.E. Varfolomeev and A.A. Vasiliev, *Sensors and Actuators B: Chemical* (1994), 19, 434.
10. G. Fan, Y. Wang, M. Hu, Z. Luo, K. Zhang and G. Li, *Sensors* (2012), 12(4), 4594.
11. Y. Yang, H. Ma, J. Zhuang and X. Wang, *Inorganic chemistry* (2011), 50, 10143.
12. N.V. Long, Y. Yang, M. Yuasa, C.M. Thi, Y. Cao, T. Nann and M. Nogami, *RSC Adv* (2014), 4, 8250.
13. N.V. Long, Y. Yang, C.M. Thi, Y. Cao and M. Nogami, *Colloids and Surfaces A: Physicochemical and Engineering Aspects* (2014), 456, 184.
14. P. Samarasekara, *Chinese Journal of Physics* (2009), 47(3), 361.
15. P. Samarasekara, *Georgian Electronic Scientific Journals: Physics* (2010), 2(4), 3.
16. P. Samarasekara and N.U.S. Yapa, *Sri Lankan Journal of Physics* (2007), 8, 21.
17. P. Samarasekara, A.G.K. Nisantha and A.S. Disanayake, *Chinese Journal of Physics* (2002), 40(2), 196.
18. K. Tennakone, S.W.M.S. Wickramanayake, P. Samarasekara and, C.A.N. Fernando, *Physica Status Solidi (a)* (1987), 104, K57-K60.
19. P. Samarasekara and Udara Saparamadu, *Georgian electronic scientific journals: Physics* (2012), 1(7), 15.
20. P. Samarasekara and N.H.P.M. Gunawardhane, *Georgian electronic scientific journals: Physics* (2011), 2(6), 62.
21. P. Samarasekara, *Electronic Journal of Theoretical Physics* (2008), 5(17), 227.
22. P. Samarasekara and Udara Saparamadu, *Research & Reviews: Journal of Physics-STM journals* (2013), 2(2), 12.
23. P. Samarasekara and Udara Saparamadu, *Georgian electronic scientific journals: Physics* (2013), 1(9), 10.
24. P. T. Moseley, J. Norris and De Williams, *The Adam higher series on sensors publishers* (1991).
25. S. Chopra, K. McGuire, N. Gothard and A.M. Rao, *Applied Physics Letters* (2003), 83, 2280.

26. L. Li, Z. Tong, L. ShouChun, W. LianYuan and T. YunXia, Chinese Science Bulletin (2009), 54, 4371.
27. W. XiuZhi, Chinese Science Bulletin (2012), 57, 4653.
28. N. Yamazoe, Sensors and Actuators (1991), B 5, 7.
29. G.F. Fine, L.M. Cavanagh, A. Afonja and R. Binions, Sensors (2010), 10, 5469.
30. C.R. Michel, A.H. Martinez, F.H. Villalpando and J.P. Moran-Lazaro, Journal of Alloys and Compounds (2009), 484, 605.
31. C.V. G. Reddy, S.V. Manorama and V.J. Rao, Journal of Materials Science Letters (2000), 19, 775.
32. P. Samarasekara, M.S.P.K. Gunasinghe, P.G.D.C.K. Karunarathna, H.T.D.S. Madusanka and C.A.N. Fernando, Georgian electronic scientific journals: Physics (2019), 1(21), 7.
33. Y. F. Sun., S. B. Liu, F. L. Meng, J. Y. Liu, Z. Jin, L. T. Kong, and J. H. Liu, Sensors (2012), 12(3), 2610.
34. J. Zhang, Z. Qin, D. Zeng and C. Xie, Physical Chemistry Chemical Physics (2017), 19(9), 6313.
35. B. Cui, T. Li, J. Liu and M. Marinescu-Jasinski, Materials Research Express (2015), 2, 045011.

Article received: 2019-07-15